Does Morphology Stick? Tailored Particle Morphologies by Swelling Polymerization Process

S. Kirsch,[1] M. Kutschera,[2] N.-Y. Choi,[2] T. Frechen[2]

[1]*BASF AG, Product Development Adhesives and Fiber Bonding, D-67056 Ludwigshafen, Germany*
[2]*BASF AG, Polymer Research Laboratory, D-67056 Ludwigshafen, Germany*

Received 25 August 2005; accepted 10 January 2006
DOI 10.1002/app.24076
Published online 4 May 2006 in Wiley InterScience (www.interscience.wiley.com).

ABSTRACT: Structured dispersion particles suitable for pressure sensitive adhesives (PSA) were synthesized via swelling polymerization technique (EP 359562). Particles consisting of poly(*n*-butyl acrylate) copolymerized with different types of carboxylic acids were used as seeds. The final particles were synthesized by swelling polymerization process, using 6 wt % styrene or 6 wt % methyl methacylate. The resulting particle morphology was analyzed by atomic force microscopy (AFM) and transmission electron microscopy (TEM). From previous works (Coll Surf A 2001, 183–185, 725–737; J Appl Polym Sci 2004, 91, 2610–2623) where two-step emulsion polymerization was used on similar particles, it is expected that the particle morphology is affected by the polarity of the monomer used for swelling polymerization because of the phase compatibility (thermodynamic parameter). In this work, the seed particles used were always of a glass transition temperature (T_g) below polymerization temperature. The diffusion of the growing polymer chains from the swelling polymerization is therefore mainly affected by their own T_g and the influence of the carboxy groups on the chain length of the entering radicals (kinetic parameter). The different morphologies of the single particles are discussed qualitatively. The effects of reaction parameters are compared with the results given in the previous work. The structure of the corresponding dispersion films was characterized using AFM. Correlations to macroscopic properties such as the cohesive strength and peel adhesion to different substrates are discussed. The results are also compared with the application properties of the corresponding unmodified particles, statistical copolymers, and to blends with small sized PMMA or PS particles. © 2006 Wiley Periodicals, Inc. J Appl Polym Sci 101: 1444–1455, 2006

Key words: adhesives; atomic force microscopy (AFM); emulsion polymerization; morphology; TEM

INTRODUCTION

Acrylic dispersions are used since the early fifties for pressure sensitive adhesive (PSA) films. Nowadays, many products, such as tapes, filmic and paper labels are based on this technology.[1,2] Albeit there are specific requirements for each application, three basic properties have to be optimized: (i) shear strength,[3] which is the ability to withstand a static shear force, (ii) peel adhesion, which is the force required to peel the adhesive under a certain angle from the substrate, and (iii) tack,[4,5] which means the force to break a bond after short contact time and low contact pressure. In many applications of PSAs, not only a high tack but also a high cohesion (even at high temperatures) is required. For example, tapes used in the automotive industry or paper labels used in laser printers. Usually, the tack is decreased when the density of physical entanglements is increased. At the same time, the cohesion is increased because of the reduced viscous flow of the polymer. One strategy to overcome this relationship is to use dispersion particles, which are structured on a nanometer scale.[6] Dispersion particles with tailored morphology are also known as binders used in modern, water-based industrial applications such as paints and coatings.[7–10] For paints, film forming without coalescent agent but high surface hardness is an example, where similar contradictory requirements have to be covered. For all these needs, the concept of tailored particle morphology, which is a special arrangement of two polymer phases within one particle, was developed. Thus, latex film properties can be achieved, which are different from what can be achieved by physically blending two or more different polymer components.[11] In addition, special interaction phenomena of phase-separated particles to various substrates may occur.[12,13]

From that point of view, it is of great interest to understand how particle morphology can be controlled. Much work has been described in literature on how phase-separated particles can be synthesized via a two-step emulsion polymerization. Furthermore, work is published on theoretical models and simulation tools to understand and predict the formation of structured particles.[14–17] Particle structures generated by a two-step emulsion polymerization are usually in

Correspondence to: S. Kirsch (stefan.kirsch@basf.com).

the range of several tenths of nanometers, depending on the stage ratio used[9,10,18]. These structures are very useful when the dispersion is used as a binder for paints.[7,8] For adhesives such large domains would negatively affect tack and peel strength in a very dominant way. To achieve small domain sizes, the swelling polymerization process[19–21] seems to be a suitable pathway. This process comprises a complex variety of process parameters, e.g., feeding time of the swelling monomer, swelling time, and type of initiator used to restart the polymerization. Using different monomers with different polymer glass transition temperatures (T_g) or different polarities allows one to achieve specific particle morphologies. Parameters to be considered in controlling the particle morphology can be divided into two types: (i) Thermodynamic factors: the resulting morphology is driven by the contribution of the surface free energy. The surface free energy can be affected, for example, by the type and amount of monomer used during swelling as well as the type and amount of initiator used to restart the process. Quantitative guidelines and methods to predict the equilibrium morphology are reported elsewhere.[22,23] (ii) Kinetic factors: the resulting particle morphology is controlled by diffusion and phase rearrangement within the particles. The mobility of the polymer chains is restricted and hence phase separation and rearrangement are slower than the polymerization rate. The mobility of the radical chains can be strongly affected by the monomer concentration within the particles (and hence the swelling time), the T_g of the polymer resulting from the swelling step, and the difference to the reaction temperature.

Compared to the parameters described so far, only little attention was given to the effect of carboxylic acid.[24] In industry, the most common carboxylic acids are acrylic acid (AA), methacrylic acid (MAA), and itaconic acid (IA). From the current understanding, it is clear that the effect of carboxylic acids can neither be attributed to the thermodynamic nor to the kinetic condition alone. In fact, they affect morphology through both factors. It is known that by a surface layer of carboxylic acid on a dispersion particle, the radical flux (entry and exit) is affected.[25] In addition, the length of entering radicals is increased when acid comonomers are used, which reduce their ability to diffuse into the seed particles. Additionally, surface free energy, and therefore the equilibrium morphology, between polymer phases is also modified when hydrophilic groups, e.g. acid comonomers[26,27] or sulfate groups from the initiator, are incorporated into the polymer chains. Effects of the various types of carboxylic acids are not discussed until now.

In the current work, a swelling polymerization process was used to synthesize structured particles. Low T_g particles of carboxylated poly(*n*-butyl acrylate) (PnBA) were used as seeds. In the second stage, pure PMMA or PS was polymerized via a swelling polymerization step to build up high T_g hard phase domains. The phase ratio of soft seed to high T_g monomer was fixed at 6wt% of the swelling monomer. Furthermore, the effect of the type of carboxylic acid on the resulting particle structure was investigated by copolymerizing acrylic-, methacrylic-, or IA within the seed particles.

Different characterization tools are available to characterize the particle morphology of latex particles.[28] In this work, two different techniques were used.

i. Atomic force microscopy (AFM) was used to characterize the structure of the current latex system. Because of the difference in T_g, it is possible to map a material contrast by taking advantage of differences in viscoelastic properties of different phases using "phase imaging."[29,30] Spatial resolutions below 10 nm can be routinely achieved on the investigated polymer system.
ii. Transmission electron microscopy (TEM) was used for all samples where styrene has been used as swelling monomer. Here, staining with RuO_4 is a well-established technique, which allows mapping a chemical contrast.

Important aspects of this work are as following: first, to characterize and to discuss the resulting particle morphology of the particles obtained via swelling polymerization process within the framework of thermodynamic and kinetic considerations as discussed in previous work.[9,10] Second, to correlate the dispersion film structure of four different sets of samples to their macroscopic adhesive properties i.e., cohesive strength and peel adhesion to different substrates.

EXPERIMENTAL

Equipment

All syntheses were performed in a 1000-mL three-necked reactor equipped with a reflux condenser, N_2-gas inlet tube, anchor-stirrer stirring at 160 rpm, inlet tube to feed the pre-emulsion, and a feeding tube for the initiator solution.

The particle size distributions of the samples were examined by analytical ultracentrifugation (AUC) in sedimentation velocity runs. The AUC is based on a preparative OPTIMA XL (Beckman, Palo Alto) and equipped with a turbidity detector.

The T_g was measured with a DSC822 (TA8000) from Mettler-Toledo. The midpoint from the second heating curve (20°C/min) was determined.

Synthesis and particle characterization

Four different sets of dispersion systems were under investigation: (i) Seed particles: bimodal PnBA parti-

cles polymerized by a conventional semibatch emulsion polymerization process without copolymerizing MMA or styrene. (ii) Statistical copolymers: standard recipe as before but now copolymerizing 6 wt % MMA or styrene. (iii) Swelling copolymers: seed particles prepared by process (i) and then swelling polymerization of 6 wt% styrene or MMA was conducted. (iv) Blends of 94 wt% seed particles of system (i) and adding 6 wt% 27-nm-sized PS or 19-nm-sized PMMA particles.

The bimodal PnBA latex particles of types (i) and (ii) were prepared as follows: for the initial charge, 85 g deionized water and 50 g of the initiator solution (7% aqueous solution of sodium peroxodisulfate) were flushed with N_2 and heated to 65°C. At 65°C, the feed of a mixture of 4.67 g of 15% aqueous NH_3 solution and 10.5 g of 10% aqueous solution of sodium hydroxymethylsulfonate was started, lasting 190 min, and the temperature was raised to 80°C in 20 min.

After 10 min, the pre-emulsion was fed for 3 h to the reaction mixture at constant temperature. For type (i) the pre-emulsion was prepared from 197 g deionized water, 15.6 g Dowfax 2A1 (45% aqueous solution), 0.35 g of *t*-dodecylmercaptane, 70 g ethylacrylate (EA), 10.5 g carboxylic acid (either MAA, AA, or IA), and 578 g nBA. For type (ii) (statistical copolymer), the pre-emulsion was prepared using 42 g of styrene or MMA and 536 g nBA.

The bimodal PnBA latex particles type (iii) were prepared as follows: for the swelling polymerization process, 42 g of either styrene or MMA was fed for 15 min, starting 10 min after the completion of the monomer feed. Swelling time was 15 min. Before adding the monomer for swelling polymerization, the following amounts of residual monomers of the first stage were measured: in the case of MAA and AA containing samples, about 3 wt % nBA and 0.3 wt % EA have been found. For the IA containing particles, the level of residual monomers were significantly higher at about 6 wt % nBA and 1 wt % EA. This has to be kept in mind when effects on the adhesive properties are discussed later on.

After the polymerization, all dispersions were neutralized with 15% aqueous NH_3 to pH 7 and then allowed to cool down to room temperature (RT). All latices were bimodal with particle size distribution centered at 200 and 700 nm as measured with AUC. T_g was about −40°C for all samples as measured with DSC.

Thus, the composition of all samples was (numbers are in weight percent of total monomer): {82.5 nBA} + {10 EA} + {0.05 *t*-dodecylmercaptane} + {1.5 MAA, AA, or IA} + {6 styrene or MMA, either by swelling polymerization/statistical copolymerization/blending}.

Atomic force microscopy

The following steps were performed to produce standardized, high quality samples for AFM characterization: A small amount of polymer dispersion was allowed to dry for several days. A cross section through the bulk of the dried dispersion was prepared by cryo ultramicrotomed cutting. Special attention was paid when defrosting the samples back to RT to avoid both condensation onto the fresh surface and segregation of still liquid components from the bulk.

All AFM measurements presented in this work were performed at ambient conditions (air, RT, r.h. ~40%) with a Digital Instruments Nanoscope Dimension 3000 SPM. The system was equipped with a phase extender box to allow simultaneous recording of height and phase data in tapping mode (TM) operation (Si cantilevers, 35 N/m, ~300 kHz). The parameters were carefully adjusted to operate in the stable repulsive regime (imaging frequency below the resonance frequency).

Only TM phase images are presented, as the microtomed surfaces were nearly ideally flat ($\Delta z \ll 10$ nm). The inevitable fake topography signal that is created by the influence of hard and soft surface areas was in turn used for the interpretation of the contrast in the phase signal.

Transmission electron microscopy

For the investigation of the internal phase distribution of the latex particles synthesized via swelling polymerization process with styrene, TEM was used. As the particles may contain only one or a few small inclusions, it is crucial to acquire the information on the whole particle. So, the standard TEM procedure of preparing ultrathin sections of dried films is not suitable. Instead, a submonolayer of the dispersion was prepared onto a TEM grid, which contains the complete particles. To do this, a small dispersion droplet is spread on a bidestilled water surface. The dispersion particles rearrange spontaneously forming a submonolayer, which can be easily picked up with the TEM grid. This procedure includes a partial purification of the dispersion, as water-soluble species (such as surfactants) diffuse into the water phase. A disadvantage is that soft particles may broaden making it difficult to measure their correct size.

The TEM investigation of polymer phases requires selective staining with heavy metal compounds. With the particle size in the range of 200–700 nm, the bulk of the particles should be transparent for electrons to enable TEM at operating voltages in the range of 80–120 kV. So, the internal styrene phase was stained with RuO_4, leaving the bulky acrylic phase unstained. The RuO_4 solution was prepared from 5 mL aqueous NaOCl (~13% active chlorine) and 0.1 g $RuCl_3$, ac-

cording to Ref. 31. For staining, the dried TEM grid with the latex particles was kept next to an open vessel with the RuO_4 solution for 20 min at RT, enabling the reaction with RuO_4 vapor. Furthermore, to label the particle boundary, prior to the submonolayer preparation, the latex particles were stained with a 2 wt % aqueous solution of uranyl acetate, which was added to the wet dispersion. Reaction time was 2 min. Uranyl acetate stains the acidic groups, which usually cover the surface of the latex particles. TEM examination was performed with a LEO 912 Omega at 120 kV. In the TEM micrographs, the stained parts of the polymer particles appear dark.

The information obtained by AFM and TEM complement each other ideally. With TEM, the phase morphology of the complete particles is recorded, provided that the phases can be stained selectively. With AFM performed at sections of a dispersion film, only a small part of a particle is accessible, but components, which are not stainable for TEM, can be identified with nanometer resolution, exploiting various contrast mechanisms in the AFM addressing hardness, friction, or chemistry.

Adhesive properties of the dispersion films

For all samples, application properties were tested from the neat polymer as well as from the formulated one. For formulation, 20 wt % of rosin ester (based on polymer content) was added. The rosin ester (tackifier) is used to enhance the mobility of polymer chains, resulting in a higher loop tack and peel adhesion but lower cohesion of the adhesives. To enhance the adhesion, specific interaction of the tackifier to the polymer chain is required. In Ref. 32, the modification of acrylic latices by resin and the resulting effects are described in detail. In addition, 1 wt % of dioctyl sulfosuccinate (DOSS) to ensure the ability for transfer coating via siliconized paper was used. DOSS also lowers the cohesion of the adhesive in a significant way but does not contribute to the adhesion.

The coating weight was adjusted to 19 g/m^2. The cohesion from the resulting paper labels was determined according to FINAT test procedure FTM 8. The peel adhesion after 1-min dwell time to steel, PE, and corrugated cardboard was determined according to FINAT test procedure FTM 1.

RESULTS AND DISCUSSIONS

Proposing that microstructures in dispersion films introduced by high T_g polymer phases are of advantage for the balance between cohesion and adhesion of a given system,[19] swelling polymerization process was used to "preform" these structures in the dispersion particles. In the first part of this section, we focus on theoretical aspects to tailor particle morphology and the characterization of single particle and particle film morphology by TEM and AFM. Our aim was to evaluate the effect of both the polarity of the first-stage polymer by using different types of carboxylic acids and the polarity of the swelling monomer on their resulting particle and film structures. In the second part, we focus on the investigation of application properties and their correlation to single particle and polymer film structures.

Structure of single particles

In Refs. 33 and 34, simulation tools were presented to predict the morphologies of single particles by considering thermodynamic and kinetic factors. In Refs. 9 and 10, these tools have been used to describe a straight acrylic system. In Refs. 9, 10, and 24, effects of carboxylic acids on the particle structure have been discussed. Taking this into account, the following structures would be expected: from the thermodynamic point of view, the relation of the surface tension of the polymer to the water phase and the polymer/polymer interaction plays the major role. From this, it is expected that one PS domain is formed inside a PnBA particle because of its higher hydrophobicity and the incompatibility of the polymers, forcing the system to a small contact area (inverse core-shell). Following the same arguments, PMMA being the more hydrophilic polymer compared to PnBA should stay at the outside. Because of a higher compatibility of the two polymers core–shell morphology would be favored instead of a half-moon structure. In addition, the concentration of residual monomer has to be taken into account. This also lowers the driving force of phase separation of the polymers, because a certain degree of the first-stage composition is copolymerized. Deviations from the thermodynamically favored structures can only be introduced by the effect of the kinetic factor, which is based on a limited diffusion of second-stage polymer by increased local viscosity. In the given system, this could be due to the carboxylic acid because the first-stage polymer is always well above T_g. It is well known that compared to AA, MAA is more incorporated within the particles, while IA is more or less located in the aqueous phase. Thus, less effect of the more polar IA on the particle structure of the PS system predicted by the thermodynamic considerations is expected. As the PMMA phases are expected at the particles surface, the concentration of carboxylic groups at the particle surface should have a strong influence on the structure of this system. Again, for the IA, we expect the smallest effect, leading to the largest PMMA domains. For MAA and AA, the partitioning in the particle and at the surface is relevant. As no data on the partitioning for our system are available, we can only propose to find domains of smaller size.

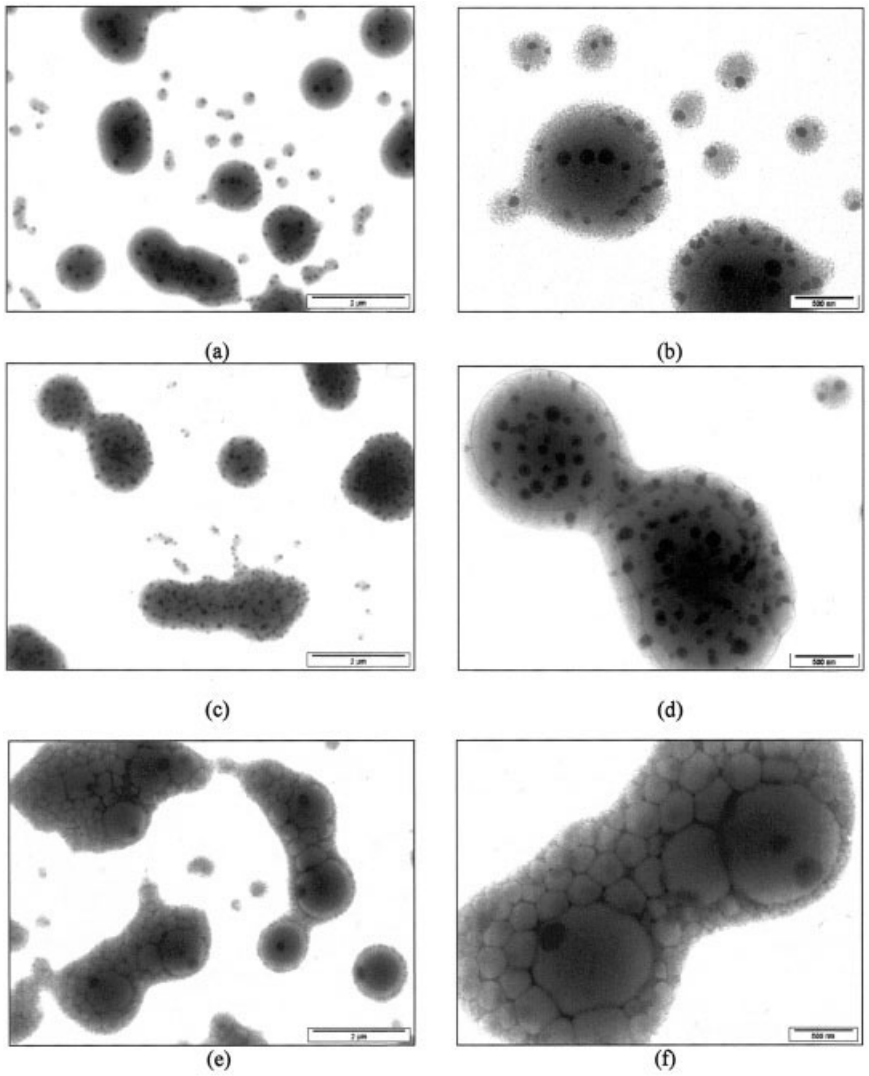

Figure 1 TEM images of PnBA seed particles combined with swelling polymerization of styrene: (a, b) copolymerized with AA, (c, d) copolymerized with MAA, and (e, f) copolymerized with IA.

Characterization of single particle morphology by TEM

The TEM images in Figures 1(a–f) show the latex particle morphology of a series of bimodal PnBA dispersion particles after swelling polymerization process with 6 wt % styrene. The particles are partly aggregated because of preparation. With both, AA and MAA [Figs. 1(a–d)], the PS forms multiple domains within the large dispersion particles. There seem to be more PS domains present in the case of MAA-containing particles compared with those in the AA counterparts. In the small dispersion particles in all cases only one or two PS domains are present. In contrast, with IA [Figs. 1(e,f)] the PS is concentrated only in one domain.

The size of the PS domains in the large particles varies in the dispersions with AA and MAA in a range from about 30 to 120 nm. In the dispersion particles with IA, the PS domains are larger and more uniform with about 200 nm in size (compare also Table I).

Structure of the dried dispersion film

AFM was used to characterize the morphology of the dispersion films. Figure 2 shows a typical cross section through a dried polymer dispersion film. The bimodal PnBA dispersion particles (170 nm/750 nm) appear as more or less circular dark patches. Light and dark areas in the phase images correspond to negative and positive physical phase shift of the oscillating cantilever, respectively. The coalescence forces during drying cause the slightly irregular shape of the polymer particles when water evaporates and the polymer particles approach each other. Therefore, the additives of the liquid phase such as salts, stabilizers, or emulsifiers are accumulated between the particles. These ad-

TABLE I
Particle Sizes of the Swollen Polymer Domains as Detected by the TM-AFM Cross-Section Images

Carboxylic acid/swelling monomer	MAA	AA	IA
Styrene	25 nm/110 nm	20 nm/100 nm (very few)	30 nm
Methyl methacrylate	20 nm/70 nm (few)	60 nm	30 nm/120 nm (few)

ditives lead to the faint yellow particle boundary network or crystallize to hard entities clearly visible as bright spots in Figure 2. From Ref. 9, it is known that for systems with a polymer phase with a T_g significantly higher than RT the single particle structure is maintained during the process of film formation. It is then easy to identify the PS or PMMA domains as light-colored spots within the dark areas.

Variation of swelling monomer

We turn now to the results given in Figure 3. In the second row, the results on dispersion films are given with styrene incorporated by the swelling polymerization process. Starting with AA, we observe faint hard polystyrene domains inside the polymer particles, most of them very small and only a few bigger ones. (For the dimensions of the swollen domains refer to Table I). With MAA a true bimodal distribution of swollen domains are created, whereas IA leads to one single PS domain inside the particles. By means of these particles created with IA, we can clearly show that investigating dispersion particles with only one method will inevitably lead to misinterpretations. In this special case, the single PS phase inside the PnBA matrix can be easily missed while cross sectioning the particles and not directly hitting them. This is due to the high (~nm) surface sensitivity of the AFM method, which prohibits looking below the surface. Together with the help of TEM microscopy, which probes through the whole particle [see Fig. 1(f)], the real morphology can be determined. It is important to point out that these hard swollen styrene domains are only created within the soft (hydrophobic) polymer particles. This can be seen in TM-AFM images of the film surface (Fig. 4, left) where no hard domains are found on the particle exterior.

In the third and last row of Figure 3, the results from swelling polymerization with MMA are depicted. Here again swollen domains are created within the polymer particles. But in contrast to styrene some of the PMMA domains are also located at the surface of the polymer particles (Fig. 4, right). As expected, this is a result of the increased hydrophilicity of the swell-

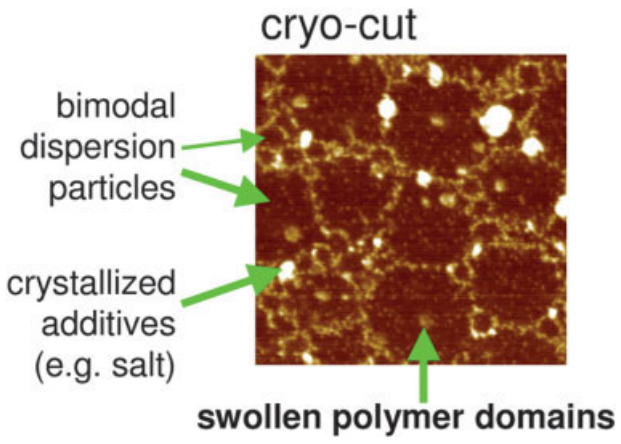

Figure 2 Typical TM-AFM phase image (2 μm × 2 μm, $\Delta\theta$ = 20°) of a cross section through a dried polymer dispersion film. The individual bulk features are labeled. [Color figure can be viewed in the online issue, which is available at www.interscience.wiley.com.]

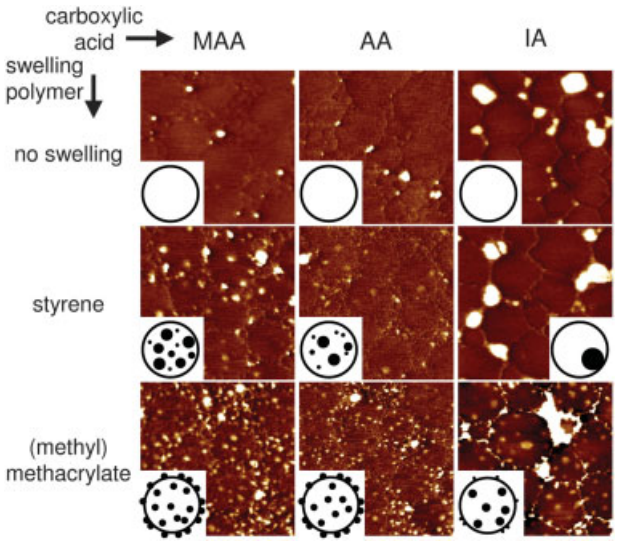

Figure 3 Cross sections of dried dispersions with different chemical composition and morphology [TM-AFM phase images, 2 μm × 2 μm]. Different columns hold dispersions with different carboxylic acids, whereas the changes implied by swelling polymerization are shown in different rows. The insets are used to schematize the observed particle morphology. [Color figure can be viewed in the online issue, which is available at www.interscience.wiley.com.]

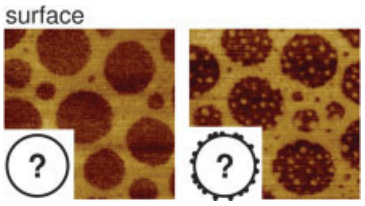

Figure 4 Surfaces of dried dispersions with MMA (right) and styrene swelling (left) [TM-AFM phase images, 2 μm $\times$ 2 μm]. The hard (bright) spots on the right side are the swollen MMA domains sitting on the surface of the dark polymer particles. These spots are missing in the left image, indicating that styrene is not on the surface but inside the dispersion particles. [Color figure can be viewed in the online issue, which is available at www.interscience.wiley.com.]

ing monomer. In contrast to the PS system, these hard domains could contribute to a mechanical stability of both the PnBA-particles themselves and of the particle network.

To conclude this discussion, we have shown that with a second swelling step using MMA as monomer it is possible to create very small PMMA domains at the surface of the existing PnBA particles. With the help of a compatible carboxylic acid (AA or MAA), these small hard domains can be synthesized numerously and evenly distributed at the surface and in the inside of the main PnBA particles. The structures found by TEM and AFM analysis are in good agreement to the structures we expected from the theoretical point of view that we have discussed at the beginning of this section.

Variation of carboxylic acid and effect on the interstitial film structure

For the effect of using different carboxylic acids during emulsion polymerization, we refer to the images in the first row of Figure 3. Here, it gets obvious that—-apart from particle size effects—-the changes in acids mainly influence the particle interaction during the drying process. With IA, the polymer particles appear more deformed. This indicates stronger interaction forces during the drying process. On the other hand, the particles seem to be clearly separated from each other, which stands for a weak interdiffusion (and few entanglement) of polymeric chains from different particles. Additionally, the highly hydrophilic acid causes a strong separation of the polymeric (hydrophobic) versus the serum (hydrophilic) phase. This is a reason for the distinct and wide stretched hard (bright) areas of crystallized additives.

For the interpretation of the application properties, we have to keep this general effect on the film structure in mind. Starting from MAA to AA and IA, the hydrophilicity level of the acid is increased and thus the concentration of water-soluble substances is increased. It is expected that in the adhesive film, the accumulation of low molecular weight but high T_g material between the polymer particles results in increased cohesion and accumulation on the film surface in a decreased adhesion especially to nonpolar substrates.

Correlation to macroscopic properties

For the application tests of the corresponding adhesives, three different substrates have been used: nonpolar PE, polar steel surface, and corrugated cardboard with an average surface roughness of $\pm$30 μm (determined by a laser profiler). In Figures 5 and 6 the adhesive properties of the formulated systems are shown in detail. The average performance of the neat polymer is given as dotted lines for comparison in each case. The deviations in peel adhesion span a range of only $\pm$2 N/25 mm.

In Figure 5, the results of application testing of the "PS" system (film structures varied by introducing PS domains) are shown. Considering the cohesive properties [Fig. 5(d)], the following interpretation is given.

i. Compared to the reference without styrene (circles), the samples copolymerized statistically with 6 wt % styrene (squares) show a tremendously lower cohesion. This is due to the fact that styrene is affecting the rate of polymerization. The conversion is lower, and hence at a constant feed rate, the emulsion side reactions, which lead to gel formation in the polymer particles, are less numerous. As microgel or domains with high content of physical entanglements are responsible for high cohesion, the cohesion drops. The cohesion is not significantly affected by the polarity of the comonomers.
ii. In the case of structured particles (diamonds), the level of cohesion is higher compared with that of the latter samples, as expected. This is due to the PS domains, which act as stiffeners because of the immobilization of the polymer chains at the interface. The cohesion compared to the reference (circles) is again on a lower level. This can be explained by the level of residual nBA at the start of the swelling process, which is now reacting like discussed in (i). Again, the polarity of the resulting polymer has no significant effect on the cohesion.
iii. For the samples blended with small sized PS particles, a trend to higher cohesion with higher polarity can be observed. This can be attributed to a distribution effect of the PS particles. Higher amounts of water-soluble oligomers might act as a disperant for the dispersion particles. A better distribution would lead to higher cohesion,

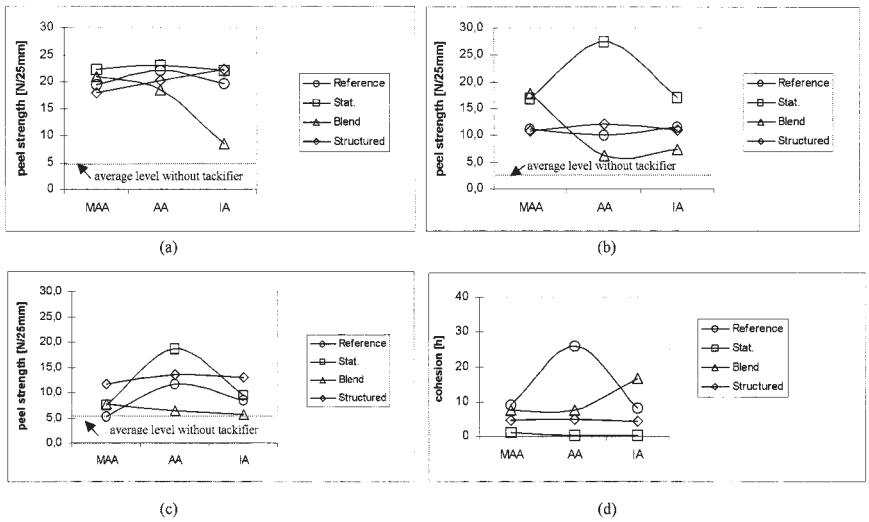

Figure 5 Application properties of tackified adhesive films as a function of polarity of the former dispersion particles using MMA, AA, or IA as comonomers. Film structure was varied by blending with 6 wt % PS particles (triangle), swelling polymerization with 6 wt % styrene (diamond), and comparing references without high T_g polymer (circles) and a films of particles copolymerized with 6 wt % styrene (squares). The adhesive properties were tested as peel adhesion [N/25 mm] after 1-min dwell time on different substrates: (a) polar, low surface roughness steel; (b) nonpolar, low surface roughness PE; (c) medium polar but high surface roughness corrugated cardboard; and (d) the time to failure of the bond to steel applying 1 kg weight was recorded in hours for cohesive measurement.

whereas an aggregation of the PS particles or enrichment at the surface during the process of film formation would lower the cohesion. The higher level of cohesion compared to the structured particles was initially not expected. A chemical grafting of the hard phase domains should lead to a higher mechanical strength compared with that of the corresponding blend.

iv. The reference samples (circles) are on a high level of cohesion. This is due to the fact that no styrene is copolymerized with the discussed effects on the structure of the polymer

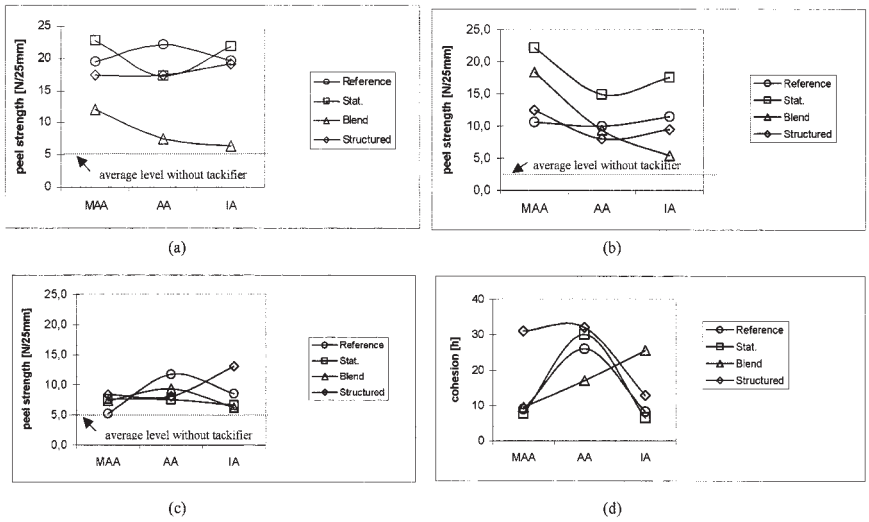

Figure 6 Application properties of tackified adhesive films as a function of polarity of the former dispersion particles using MMA, AA, or IA as comonomers. Film structure was varied by blending with 6 wt % PMMA particles (triangle), swelling polymerization with 6 wt % MMA (diamond), and comparing references without high T_g polymer (circles) and a films of particles copolymerized with 6 wt % MMA (squares). The adhesive properties were tested as peel adhesion [N/25 mm] after 1-min dwell time on different substrates: (a) polar, low surface roughness steel; (b) nonpolar, low surface roughness PE; and (c) medium polar but high surface roughness corrugated cardboard; and (d) the time to failure of the bond to steel applying 1 kg weight was recorded in hours for cohesive measurement.

chains. From the results given in (i) and (ii), a dependency on the polarity is not expected, but especially the sample copolymerized with AA is significantly higher in cohesion. This effect is not clear to us yet and does not correspond to the results of adhesion we discuss later on.

Keeping the cohesive properties in mind, the adhesion to different substrates has to be discussed. The results are given in Figures 5(a–c). The following interpretation can be given.

i. The adhesion to steel [Fig. 5(a)] as a polar substrate is mainly affected by the use of tackifier. The average adhesion is raised from 5 to 20 N/25 mm where for all samples an adhesion failure for the neat polymer and a failure of paper tear for the formulated polymer were found. The tackifier enables the polymer chains to exhibit a higher mobility. Thus, orientation for specific ionic interaction to the polar substrate is provided. Presuming that the wetting and creep properties are on a certain level, it is clear that the force of adhesion is within a relatively narrow range for all samples. Beside this major effect details can be discussed taking the cohesion into account. From this, it is clear that the samples with 6 wt % statistically copolymerized styrene (squares) are on the highest level of adhesion. Compared to this, the adhesion of the reference (circles) is expected to be on a slightly lower level. The trend of adhesion for the blend (triangles) is opposite to its cohesion. Here, we found the sample containing IA on a very low level of adhesion, which leads to the assumption that there was an enrichment of the hydrohopbic PS particles at the interface to the hydrophobic air during the process of film formation. This could contribute to less sticky areas. The result for the structured particles (diamonds) is interesting. Here, we can observe a slight dependence on the type of acid used. The higher the hydrophilicity, the better is the adhesion. This could be attributed to a kind of direct interaction with the higher amount of polar groups at the surface of the film in the case of IA. To explain the slightly lower level of adhesion for the samples with MAA and AA in comparison with the reference and the statistically copolymerized samples, the structure given in Figure 3 has to be considered. For the IA containing particles, we found only a low amount of large domains. The fact that a higher number of small domains lead to a higher portion of interface leads to the conclusion that the interface polymer chains are immobilized[18] and creep properties are affected in a negative way. Nevertheless the sample with the structured particles containing IA has the best balance between cohesion and adhesion to steel.
ii. The adhesion to PE as a nonpolar substrate [Fig. 5(b)] is more diversified than the adhesion to steel. The peel adhesion is now not only affected by formulating with tackifier, but also is significantly raised from an average level of 3 N/25 mm (adhesive failure) to an average range spanning from 7 to 20 (adhesive to paper tear failure) N/25 mm by formulating. The overall level of adhesion compared to the peel adhesion on steel is lower, as no specific ionic interaction exists. Now, mainly excellent wetting and creep properties enable van der Waals interaction controling the adhesion. Starting from this basis it is clear that again the very soft statistical copolymers (squares) show the highest peel adhesion. The significantly higher peel adhesion with AA is not clear to us yet. The peel adhesion of the reference (circles) and structured particles (diamonds) is on a significantly lower level, which corresponds to the significantly higher cohesion. As we would expect, no dependence on the type of acid used could be seen, which also means that different types of acids do not affect the compatibility to the tackifier. The samples blended with PS (triangles) follow the same trend that with increased polarity peel adhesion is decreased. This is again opposite to the cohesion of the samples. In this series, the blends are of significantly lower peel adhesion (AA and IA) than the other samples, which may be attributed to distribution effects of the small sized particles (aggregation, enrichment at the surface). From the adhesion data of this experimental set where no specific interaction is expected, we can draw the conclusion that structures built up by high T_g polymers on a length scale of 20–30 nm (blend and swelling polymerization, see Figs. 1 and 3) do not contribute to the adhesive properties of the film. Thus, the best balance between adhesion to PE and cohesion is found for the reference samples.
iii. The adhesion to corrugated cardboard [Fig. 5(c)] is even more difficult than the adhesion to PE because of the high surface roughness of the substrate. The average adhesion of the neat polymer is in the range of 5 N/25 mm and is changed when tackifier is used to a range between 5 and 15 N/25 mm. Adhesive failure was found for all samples. A more complex behavior can be seen for the statistical copoymers (squares). In contrast to steel or PE, a low cohesion and therefore high ability for wetting and creep does not lead to a high level of adhesion.

Only the AA containing sample shows high adhesion. This may be attributed to a specific interaction due to the fact that a similar dependence can be found for the reference (circles) and structured particles (diamonds). This trend is more pronounced for the statistical copolymer, where, because of the low cohesion, orientation of functional groups is easier. On the other hand, because of the interface area related to immobilization of polymer chains, this effect is less for the structured particles. Again, the blends (triangles) exhibit a similar behavior as before (PE and steel) where the sample with IA has the lowest adhesion to corrugated cardboard. This is again opposite to the cohesion of the samples. But the difference of the level in adhesion between the blended system and the other samples is more pronounced in this set. The balance between adhesion and cohesion is best for the structured particles. This may be discussed in a context that for an excellent adhesion on cardboard a certain level of cohesion and viscous flow has to be combined.

As a conclusion of the first set we can draw the following results: (i) The polarity of the polymer plays only a minor role. First, we found no specific interaction to steel or PE, and only for the adhesion to corrugated cardboard, AA seems to be favorable. Second, there is no difference in the compatibility to the tackifier, which could lead to a differentiation in adhesive properties. (ii) A statistical distribution of high T_g PS domains within the dispersion particles on a length scale larger than 20 nm does not contribute to adhesive properties. In blends where a statistically uniform distribution of PS particles is not guaranteed, even adhesion can even drop.

In Figures 6(a–d), the results of application testing of the "PMMA" system (film structures varied by introducing PMMA domains) are shown. Starting again with the cohesive properties [Fig. 6(d)], the following interpretations are given.

i. and ii. The MMA incorporated into the system has, in contrast to the PS system, now no effect on the polymerization rate. Thus, the cohesion of the different systems, reference (circles), statistical copolymer with 6 wt % MMA (squares), and structured particles by swelling polymerization with 6 wt % MMA (diamonds), are in the same range. Except for the sample with MAA/structured particle, we see a general trend that combined with AA the level of cohesion is higher. This can be addressed to the fact that now the formation of acid containing components with regard to the amount and distribution within the particle, particle surface and water phase, is directly related to the type of acid. It is known that the MAA is more copolymerized within the particles. In contrast, the AA can be found more at the surface of the particles and as water-soluble oligomers in the water phase and most of the IA is found in the water phase. This is supported by the findings of AFM given in Figure 3, where the water-soluble oligomers form different structures in-between the particles. After the process of film formation, the interstices between the particles are covered more or less by high T_g oligomers. On one side, this can provide a high cohesion by forming a network or preventing the polymer chains of different particles from interdiffusion. For the AA samples, the optimum balance seems to be achieved.

iii. For the blend system (triangles, blended with 6 wt % PMMA particles), we see the same trend as was seen in the PS system, that is with increasing hydophilicity the cohesion is increased, which probably relates to distribution effects.

Considering the cohesive properties, the adhesion to different substrates has to be discussed. The results are given in Figures 6(a)–6(c). The following interpretations can be given.

i. The adhesion to steel [Fig. 6(a)] is similar to the PS system. Again, the peel force is raised by the use of tackifier from 5 to 20 N/25 mm where for all samples an adhesion failure for the neat polymer and a failure of paper tear for the formulated polymer were found. Now the samples blended with PMMA particles (triangles) are clearly on a lower level of adhesion compared with those in the PS system. This has to be addressed to the distribution of the PMMA particles in the bulk and at the surface, as all other samples are on a significantly higher level and comparable to the PS system. As in the PS system, a trend of a linear decrease in adhesion coming from MAA to IA can be found. The differences, in detail, in peel adhesion of the reference samples (circles), statistical copolymer (with 6 wt % MMA, squares), and structured particles (swelling polymerization with 6 wt % MMA, diamonds) can be discussed in the same way as presented for the PS system. Beside the blended system, no significant dependence on the type of acid can be found. The structured particles seem to exhibit less mobility because of

the interface regions than the other samples. Hence, the peel adhesion after the short period of dwell time of 1 min is on a slightly lower level. As there is no significant advantage of the structured particles regarding cohesion, the best balanced sample would be one of the statistically copolymerized samples (squares).

ii. The adhesion to PE as a nonpolar substrate [Fig. 6(b)] is more diversified than the adhesion to steel. The overall level of adhesion compared to the peel adhesion on steel is lower, which is clear, as no specific ionic interaction takes place. In contrast to the PS system, now the samples statistically copolymerized with MMA (squares) are at similar adhesion level. But all samples have a significantly higher cohesion. Especially, the sample with AA has to be pointed out, showing an interesting balance between adhesion/cohesion level. This might be attributed to a positive interaction of the tackifier with this polymer, or polymer structure. The dependence of adhesion on the type of acid used depends only on the effect of flow properties, with the consequence that the adhesion is opposite to the level of cohesion. This dependence is less pronounced for the reference (circles) and the structured (diamonds) system. The level of adhesion is now significantly lower (but is comparable to the PS system), which cannot be explained by different levels of cohesion. Because of slightly decreased flow properties (contribution of interphase), the adhesion of the structured particles is on a slightly lower level when compared with that of the statistical counterparts. The blended samples again follow the linear trend we have seen and discussed before.

iii. The adhesion to corrugated cardboard [Fig. 6(c)] is again more difficult than the adhesion to PE. The average adhesion of the neat polymer is in the range of 5 N/25 mm and is changed when tackifier is used to a range between 5 and 10 N/25 mm, which has the tendency to be lower compared with that of the PS system. Adhesion failure was found for all samples. The differentiation in adhesive proprieties is not large enough to attribute this to structural effects. An advantage for the structured system (diamonds), as seen for the PS system cannot be stated here.

As a conclusion for the PMMA system we can draw the following results: (i) As in the case of the PS system, the polarity of the polymer plays only a minor role on the adhesion. We found no specific interaction to steel or PE, and in contrast to the PS system, none to the corrugated cardboard surface. Only the relatively high adhesion to PE combined with good cohesion could be due to a good compatibility to the tackifier. On the other hand, the type of acid plays an important role on the cohesion. Here, AA is favorable except for blends. (ii) A statistical distribution of high T_g PMMA domains within the dispersion particles, which are on a length scale of about 60 nm (Table I), does not participate to the adhesive properties. Using blends, where the statistical distribution of PMMA particles is not guaranteed, adhesion is on a significantly lower level compared with those in all other samples. From this set of experiments, looking on the overall performance, the statistical copolymers are favored.

CONCLUSION

Does morphology stick? The origin of this question was to improve adhesive properties by separating functional areas of adhesion and cohesion in an adhesive film, which are commonly correlated *vice versa*. Thus, the starting point of this work was to tailor single particle morphology with hard phase domains, which should act as organic fillers for a high cohesion. At the same time, high adhesion should be possible by a suitable low T_g matrix. To this end, structured latex particles were synthesized via a swelling emulsion polymerization process of high T_g monomers such as styrene or MMA. To tailor particle morphology, different types of carboxylic acids were used. The resulting particle and film structures were characterized using TEM and AFM. The resulting adhesives, which are formulations of the polymer, wetting agent, and tackifier, were compared to the corresponding statistically copolymerized or blended systems.

From the results of application testing, it turned out that a functional separation of adhesion and cohesion was not effective in the studied systems. The adhesion to PE is mainly affected by wetting and flow properties. AA seems to promote the adhesion to corrugated cardboard, but in all the other cases, the type of acid plays only a minor role. The cohesion in blended systems strongly depends on a homogeneous distribution of the fine-sized hard particles. If aggregation occurs, usually cohesion drops. Additionally, adhesion is negatively affected by an enrichment of these particles at the surface during the film formation process because of capillary forces. This cannot occur for structured particles where the hard phase domains are chemically grafted to the soft phase material. Advantages in cohesion were observed in the case of PMMA domains. The wetting and flow properties of these particles can be negatively affected because of the reduced mobility of the interface regions between soft and hard phases.

References

1. Urban, D.; Takamura, K., Eds. Polymer Dispersions and Their Industrial Applications; Wiley-VCH: Weinheim, 2002.

2. Urban, D.; Kirsch, S.; Schumacher, K.-H.; Torres-Llosa, J. Emulsion polymer adhesives. In Handbook of Adhesives and Sealants; Elsevier, to appear.
3. Zosel, A. J Adhes 1994, 44, 1.
4. Zosel, A. Adhes Age 1989, 10, 42.
5. Marcais, A.; Papon, E.; Villenave, J. J. Macromol Symp 2000, 151, 497.
6. Garrett, J.; Lovell, P. A.; Shea, A. J.; Vinely, R. D. Macromol Symp 2000, 151, 487.
7. Schuler, B.; Baumstark, R.; Kirsch, S.; Pfau, A.; Sandor, M.; Zosel, A. Prog Org Coat 2000, 40, 139.
8. Baumstark, R.; Kirsch, S.; Schuler, B.; Pfau, A. Farbe Lack 2000, 106, 125.
9. Kirsch, S.; Pfau, A.; Stubbs, J.; Sundberg, D. C. Colloids Surf A 2001, 183–185, 725.
10. Kirsch, S.; Stubbs, S.; Pfau, A.; Leuninger, J.; Sundberg, D. C. J Appl Polym Sci 2004, 91, 2610.
11. Tang, J.; Daniels, E.; Dimonie, V.; Vratsanos, M. S.; Klein, A.; El-Aasser, M. S. J Appl Polym Sci 2002, 86, 2788.
12. Kirsch, S.; Pfau, A.; Hädicke, E.; Leuninger, J. Prog Org Coat 2002, 45, 193.
13. Pfau, A.; Sander, R.; Kirsch, S. Langmuir 2002, 18, 2280.
14. Gonzalez-Ortiz, L. J.; Asua, J. M. Macromolecules 1996, 29, 383.
15. Gonzalez-Ortiz, L. J.; Asua, J. M. Macromolecules 1996, 29, 4520.
16. Chen, Y.; Dimonie, V.; El-Aasser, M. S. J Appl Polym Sci 1991, 41, 1049.
17. Chen, Y.; Dimonie, V.; El-Aasser, M. S. Macromolecules 1991, 24, 3779.
18. Kirsch, S.; Landfester, K.; Shaffer, O.; El-Aasser, M. S. Acta Polym 1999, 50, 347.
19. Zhao, C. L.; Roser, J.; Wistuba, E. W.O. Pat. 9,810,001 (1998).
20. Frankel, L. S.; Jones, G. L.; Winey, D. A. Eur. Pat. 1,875,05 (1985).
21. Chao, Y. H.; Smart, R. T.; Will, A. S. Eur. Pat. 3,595,62 (1989).
22. Durant, Y. G.; Sundberg, D. C. Macromol Symp 1995, 92, 43.
23. Durant, Y. G.; Sundberg, D. C. ACS Symposium Series, No. 663; American Chemical Society: Washington, DC, 1997; p 44.
24. Karlsson, O.; Caldwell, K.; Sundberg, D. C. Macromol Symp 2000, 151, 503.
25. Vorweg, L.; Gilbert, R. G. Macromolecules 2000, 33, 6693.
26. Kirsch, S.; Pfau, A.; Landfester, K.; Shaffer, O.; El-Aasser, M. S. Macromol Symp 2000, 151, 413.
27. Karlsson, O.; Hassander, H.; Wesslen, B. J Appl Polym Sci 1997, 63, 1543.
28. Kirsch, S.; Dörk, A.; Bartsch, E.; Sillescu, H.; Landfester, K.; Spiess, H. W.; Mächtle, W. Macromolecules 1999, 32, 4508.
29. Zhong, Q.; Innis, D.; Kjoller, K.; Elings, V. B. Surf Sci 1993, 290, L688.
30. Magonov, S. N.; Elings, V.; Whangbo, M.-H. Surf Sci 1997, 375, L385.
31. Robards, A. W.; Wilson, A. J. Procedures in Electron Microscopy; Wiley: Chichester, New York, 1993; Module 6:7.
32. Cronin, M. J. Adhes Age 1998, 41, 12.
33. Durant, Y.; Sundberg, D. C. J Appl Polym Sci 1995, 58, 1607.
34. Stubbs, J.; Karlson, O.; Jönson, J. E.; Sundberg, E.; Durant, Y.; Sundberg, D. C. Colloids Surf A 1999, 153, 255.